Composition and function of integrin adhesions

Zuidema, A.C.

PEAK1 Y635 phosphorylation regulates cell migration through association with Tensin3 and integrins

Published in the Journal of Cell Biology, Volume 221, Issue 8 (2022).

Alba Zuidema[1], Paul Atherton[1], Maaike Kreft[1], Liesbeth Hoekman[2], Onno B. Bleijerveld[2], Nagarjuna Nagaraj[3], Nanpeng Chen[4], Reinhard Fässler[4] and Arnoud Sonnenberg[1].

[1] Division of Cell Biology, The Netherlands Cancer Institute, Amsterdam, The Netherlands;
[2] Proteomics Facility, The Netherlands Cancer Institute, Amsterdam, The Netherlands;
[3] Mass Spectrometry Core Facility at the Max-Planck Institute of Biochemistry, Planegg, Germany;
[4] Department of Molecular Medicine, Max-Planck Institute of Biochemistry, Planegg, Germany.

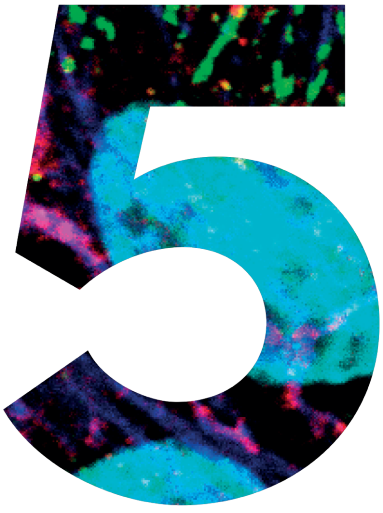

ABSTRACT

Integrins mediate cell adhesion by connecting the extracellular matrix to the intracellular cytoskeleton and orchestrate signal transduction in response to chemical and mechanical stimuli by interacting with many cytoplasmic proteins. We employed BioID to interrogate the interactomes of β1 and β3 integrins in epithelial cells and identified PEAK1 as an interactor of the RGD-binding integrins α5β1, αVβ3, and αVβ5 in focal adhesions. We demonstrate that the interaction between integrins and PEAK1 occurs indirectly through Tensin3, requiring both the membrane-proximal NPxY motif on the integrin β tail and binding of the SH2 domain of Tensin3 to phosphorylated Tyr-635 on PEAK1. Phosphorylation of Tyr-635 is mediated by Src and regulates cell migration. Additionally, we find that Shc1 localizes in focal adhesions in a PEAK1 phosphorylated Tyr-1188-dependent fashion. Besides binding Shc1, PEAK1 also associates with a protein cluster that mediates late EGFR/Shc1 signaling. We propose a model in which PEAK1 binds Tensin3 and Shc1 to converge integrin and growth factor receptor signal transduction.

INTRODUCTION

Cell adhesion to the extracellular matrix (ECM) is essential for the development and postnatal homeostasis of multicellular organisms. Cell-ECM adhesions are largely facilitated by the integrin family of adhesion receptors, which are formed through heterodimerization of an α and β subunit. Depending on the combination of the 24 α and 8 β subunits, integrins bind different ECM components, including laminins, collagens and proteins containing an arginine (R), glycine (G), aspartic acid (D) tri-peptide, such as fibronectin and vitronectin [1, 2]. Integrins link the ECM to the intracellular cytoskeleton, via a regulated network of adaptor proteins, and recruit many cytoplasmic scaffolding and signaling proteins to generate an integrated signaling network with growth factor receptors [3]. These protein complexes, known as the "integrin adhesome", play key roles in a wide range of cellular processes, including cell migration, proliferation, differentiation, and survival. Failure to properly establish cell adhesion complexes can result in severe human diseases [4].

Multiple studies have been undertaken to characterize the integrin adhesome and mechanistically understand how it drives a multitude of cellular functions in health and disease [5, 6]. These efforts resulted in an extensive literature-based adhesome protein-protein interaction network [4, 7] and a large list of adhesome components is a result of multiple proteomic studies[6]. Combining different proteomic studies generated a dataset of 60 components termed the consensus integrin adhesome [8-13]. Remarkably, only half of the proteins in the consensus adhesome are described in the literature-curated adhesome [6], indicating the need for further refinement. A powerful technology to study protein interactions at nanometer resolution in integrin adhesion sites is the proximity-dependent biotin identification (BioID) assay combined with mass spectrometry (MS)-based proteomics [14]. BioID has been used to characterize the proximity interactors of the focal adhesion (FA) proteins Paxillin and Kindlin2 [15] and to map the composition and topological features of integrin adhesion complexes by using 16 commonly identified adhesome components as bait [16]. Integration of these BioID datasets revealed a network of 147 proteins, of which only 11 proteins were identified by multiple bait proteins and most likely represent the core adhesome components [16]. We also successfully employed BioID to characterize the proximitome of integrin β4 and β5 in epithelial cells [17-19].

In the present study, we characterized the proximitome of integrin β1 and β3 and found a set of 5 adhesome components also reported in other BioID datasets [15, 16]. Among the established integrin interactors Talin1, Kindlin2, and Tensin, we also identified Kank2 and Pseudopodium-enriched atypical kinase 1 (PEAK1; SgK269). PEAK1 is a member of the PEAK family of pseudokinases, can form homo- or heterodimers with its family member Inactive tyrosine-protein kinase PRAG1 (Skg223) [20-22], and associates with

FAs and the EGFR signaling pathway [15, 16, 23-25]. How PEAK1 is integrated into FAs and whether it links FA and EGFR signaling is poorly understood. Several studies have reported elevated levels of PEAK1 and implicated PEAK1 in the regulation of tumor cell proliferation and invasion [26-32]. Furthermore, it was shown that PEAK1 is phosphorylated by Src family kinases (SFKs) downstream of growth factor receptors, which promotes its localization in FAs [23-25, 31, 33]. PEAK1 also interacts with the scaffolding protein Shc1, which occurs upon EGF stimulation with a delayed kinetics and regulates the assembly of a protein cluster involved in cytoskeletal reorganization [25]. Finally, PEAK1 has been identified as a component of the canonical Src-p130Cas-CrkII-Paxillin and Erk signaling pathways [23]. Our findings show that PEAK1 is a specific proximity interactor of RGD-binding integrins in FAs and that phosphorylation of Tyr-635 in PEAK1 regulates cell migration through association with Tensin. In turn, PEAK1 recruits Shc1 to FAs, which increases Shc1 phosphorylation, and thereby links the integrin adhesion and EGFR signaling pathways.

RESULTS

Identification of PEAK1 as core FA component

To characterize the integrin β1 and β3 proximitome by BioID (Fig. 1A), we transfected β1-null mouse epithelial GE11 cells [34] with integrin β1- or β3-BirA* cDNA and selected the bulk population of cells expressing the integrin-BirA* fusion proteins by FACS. Integrin β1- and β3-BirA* localized in FAs and β1-BirA* additionally in cell-cell contacts and in adhesion structures that resemble fibrillar adhesions (FBs)/podosomes (Fig. 1B). Cells were treated for 24h with biotin prior to cell lysis and untreated cells were used as a negative control. The use of untreated controls allowed us to normalize for any changes in protein composition resulting from expression of integrin β1 or β3. Purified proteins were run and excised from a stained polyacrylamide gel and analyzed by LC-MS/MS. Whilst we cannot rule out that the C-terminal fusion of the BirA* to the cytoplasmic tail of integrin β1 or β3 could interfere with the recruitment of some integrin-associated proteins, nevertheless, this approach resulted in datasets of 170 and 61 proteins for β1 and β3, respectively (Fig. 1C,D; Fig. S1). Amongst the top integrin proximity interactors, we found the integrin-binding proteins Talin1/2, Kindlin2 and Tensin3. Furthermore, PEAK1 and Kank2 were also among the significantly enriched proteins (Fig. 1C,D). Major differences between the β1 and β3 proximitomes were the integrin α subunits (α2, α3, α5, α6, and α7 for β1 and αV for β3) and the enrichment of CD151 in the proximity of β1 (Fig. 1E). Further comparison of the β1 and β3 datasets revealed a common set of 46 proteins (Fig. 1F; Fig. S1A), which was further compared to the proximitomes of Paxillin and Kindlin2 [15] revealing an overlap with 6 adhesome components (Fig. 1F).

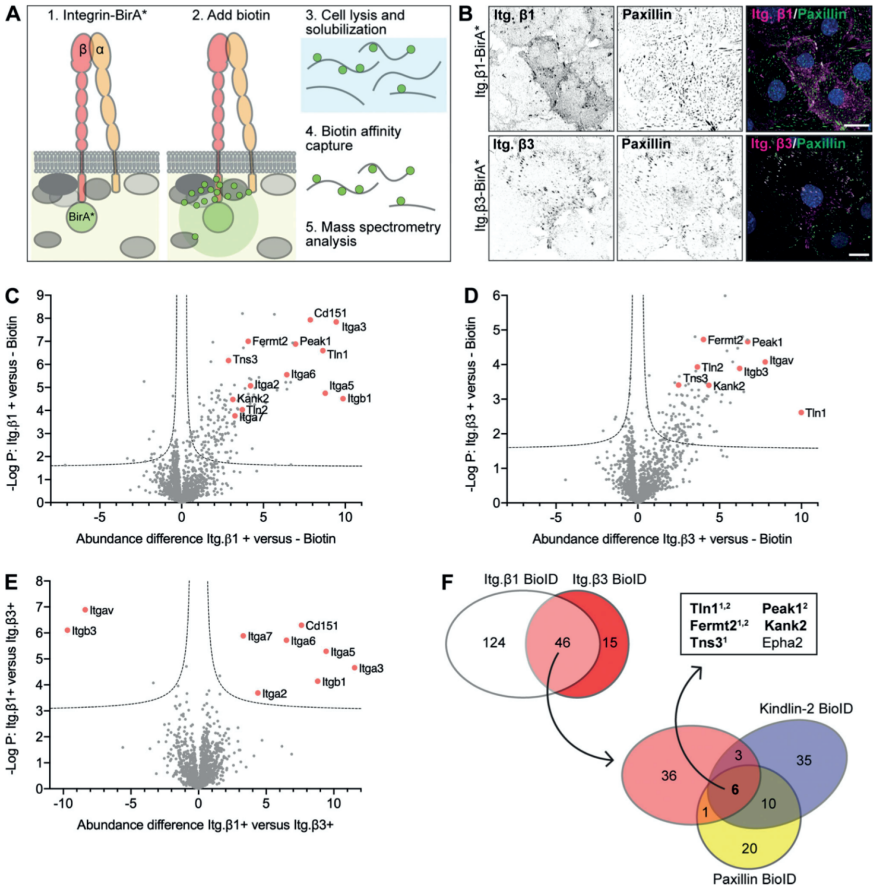

Fig. 1. Identification of PEAK1 as a proximity interactor of integrin β1 and β3. (A) Schematic depiction of the BioID assay: Integrin β subunits are tagged with the promiscuous biotin ligase BirA* on the cytoplasmic domain. Biotin is added to allow biotinylation of neighboring proteins, which are identified by mass spectrometry analysis after cell lysis and isolation of biotinylated proteins using streptavidin beads. **(B)** Integrin β1- or β3-BirA* were expressed in β1-null GE11 cells and visualized using antibodies against the β1 or β3 subunit (magenta in merge). Focal adhesions (stained with phospho-Y31 Paxillin) are shown in green and nuclei (stained with DAPI) in blue. Scale bar, 20 µm. **(C,D)** Mass spectrometry analysis of proximity interactors of β1 **(C)** and β3 **(D).** Cells were lysed after 24h of 50 µM biotin treatment. Untreated cells are used as negative control. Volcano plot shows proteins enriched in biotin-treated over control samples. The logarithmic ratio of proteins LFQs were plotted against negative logarithmic P values of a two-sided two samples t-test. The hyperbolic curve separates significantly enriched proteins from common binders (FDR: 0.05, n=4). **(E)** Volcano plot shows the proximity interactors of β1 versus β3 for samples treated with biotin. **(F)** Comparison of the proximity interactors of β1/3 and Kindlin2/Paxillin (Dong *et al.* 2016) results in 6 proteins found in all datasets. Of these 6 proteins, 5 are also identified in the integrin adhesome BioID study of Chastney *et al.* (shown in bold font). [1]: mentioned in consensus adhesome (Horton *et al.* 2015) [2]: www.adhesome.org.

Among them were proteins associated with FAs (Talin1, Kindlin2, and Tensin3) and the cortical microtubule stabilizing complex (CMSC) (Kank2) [35, 36]. Additionally, PEAK1 and EphA2 were identified in all four datasets. Talin1, Tensin3, Kank2, and PEAK1 were also identified by Chastney *et al.* using multiple FA proteins, including Kindlin2, as bait [16]. Whereas Talin1 and Kindlin2 were reported in both the consensus adhesome [13] and the literature-curated adhesome (www.adhesome.org) [4, 7], Tensin3 was only reported in the consensus adhesome, PEAK1 in the literature-curated dataset, and EphA2 and Kank2 in neither (Fig. 1E).

The identification of Talin1, Kindlin2, Tensin3, Kank2, and PEAK1 as adhesome components in multiple studies, together with their close association to integrin β1 and β3 observed in our experiments, points to their crucial role for integrin function. Because the interaction between PEAK1 and integrins is poorly understood, we decided to study this interaction.

PEAK1 interacts with RGD-binding integrins

Cell adhesion to fibronectin was shown to induce PEAK1 tyrosine phosphorylation [23]. The fibronectin dependency of this process suggests that PEAK1 associates with RGD-binding integrins. Immunofluorescence analysis of endogenous PEAK1 (Fig. 2A) or overexpression of PEAK1-GFP (Fig. 2B) in GE11/β1-BirA* cells shows that the protein localized to cell-matrix adhesions.

Integrin αVβ3 is a receptor for RGD-containing ECM proteins but β1 can heterodimerize with 12 different α subunits to additionally mediate adhesion to laminins and collagens. To study the specificity of the integrin-PEAK1 interaction, we overexpressed integrin α3-, α5-, or α6-BirA* fusion proteins in GE11 cells that also stably express integrin β1. These integrin α subunits are expressed at high levels in GE11 cells and are among the top hits in the β1 proximitome (Fig. 1C). All overexpressed integrin α BirA* constructs were expressed at the cell surface and similar levels of Itg. β1 could be detected using FACS analysis (Fig. S1B). Integrin α3β1 and α6β1 are laminin receptors, while α5β1 binds fibronectin. Overexpression of the α subunits resulted in an altered β1 subcellular distribution, with β1 localizing in FAs in the α5-BirA* expressing cells, while it shows a more dispersed organization in the α3- and α6-BirA* expressing cells (Fig. 2C), likely due to the ability of integrin α3β1 and α6β1, but not α5β1, to incorporate into tetraspanin webs through their interaction with CD151 [37].

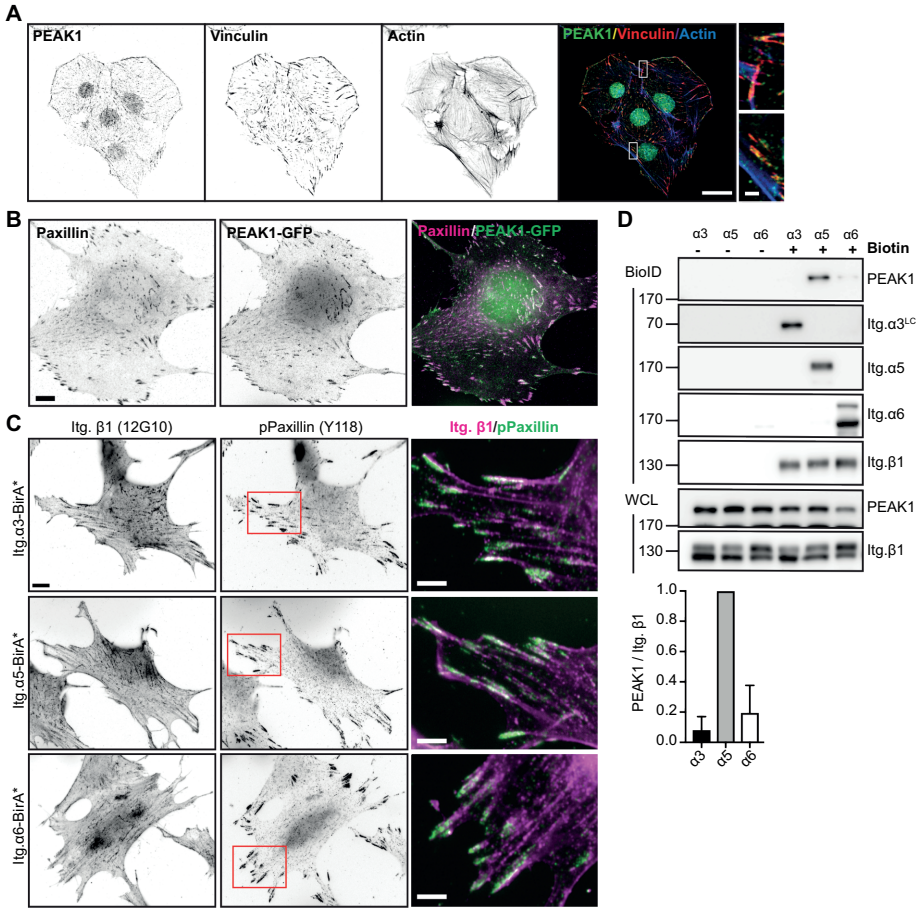

Fig. 2. PEAK1 interacts with integrin α5β1. (A) Immunofluorescence analysis of PEAK1 (green in merge), vinculin (red in merge), and actin (blue in merge) in GE11 cells expressing β1-BirA*. Nuclear localization of PEAK1 is not specific. Scale bar, 20 µm; in magnified region, 2 µm. **(B)** Overexpression of PEAK1 in GE11 Tet-ON integrin β1 cells treated with 1 µg/ml doxycycline for 48h to induce β1 expression. Scale bar, 20 µm. **(C)** Integrin α3-, α5-, or α6-BirA* was expressed in GE11 cells that stably express β1. Subcellular distribution of (active) β1 (12G10 antibody; magenta in merge) together with pPaxillin (Y118) is shown. Scale bar, 10 µm; scale bar in magnified regions, 5 µm. **(D)** Representative Western blots of the BioID assays performed using the GE11/β1 cells expressing the integrin α3-, α5-, or α6-BirA* shown in **(C)**. Cells were grown to sub-confluence in tissue plastic culture plates and treated with 50 µM biotin for 24h before cell lysis. Quantifications of PEAK1 signal intensities normalized to integrin β1 levels are shown (n=3; bars show mean with s.d.).

To examine whether PEAK1 associates primarily with the RGD-binding α5β1 integrin, we performed BioID assays combined with Western blot analysis to determine the levels of biotinylated PEAK1 in GE11 cells stably expressing integrin β1 and overexpressing integrin α3-, α5-, or α6-BirA* fusion proteins. Strong biotinylation of PEAK1 was detected in cells expressing α5-BirA*, but was absent/hardly detected in cells expressing the α3- or α6-BirA* constructs (Fig. 2D). Altogether these findings demonstrate that PEAK1 localizes in FAs and acts downstream of the RGD-binding integrins α5β1 and αVβ3.

Tensin3 links PEAK1 and integrins

Many adaptor proteins engage with the conserved membrane-proximal (MP) NPxY or membrane-distal (MD) NxxY motifs on the cytoplasmic tail of integrin β subunits [38]. For example, the MP-NPxY is required for the interaction of Talin1 with the integrin β1/3 subunit, while the MD-NxxY motif is needed for Kindlin2 binding [39]. PEAK1 does not contain an integrin-binding FERM or PTB domain found in other proteins that interact with the MP-NPxY or MD-NxxY motifs [23]. Therefore, we hypothesized that the interaction between PEAK1 and integrin β subunits might be indirect through an adaptor protein. To further examine the PEAK1 – integrin interaction, we generated β1- and β3-BirA* fusion proteins carrying disruptive Y>A mutations in the MP-NPxY (termed "N1"), MD-NxxY (termed "N2"), or both (termed "N1+2") (Fig. 3A). These mutants were stably expressed in β1-null GE11 cells; FACS analysis confirmed that all the mutants were expressed at the cell surface at similar levels (Fig. S1C). The generated cell lines were used to perform BioID combined with MS (Fig. 3B,C). Our experiments revealed that the proximity of Talin, Tensin3, and PEAK1 to β1/3 was strongly impaired when the MP-NPxY was mutated, and reduced when the MD-NPxY was mutated. These results were confirmed by performing BioID assays in combination with Western blot analysis (Fig. 3D,E). To determine which integrin MP-NPxY motif interacting protein could mediate the PEAK1-integrin association, we depleted established interactors of the integrin MP-NPxY motif by using siRNAs and subsequently studied the effects on the integrin-PEAK1 interaction by BioID and Western blot. Interestingly, knockdown of Talin1/2 or Filamins [38, 40] did not reduce the integrin β1-PEAK1 proximity interaction (Fig. S1D). We therefore wondered whether the proximity interaction between RGD-binding integrins and PEAK1 could be mediated by Tensin3, which contains a C-terminal PTB domain shown to interact with the integrin MP-NPxY domain [38, 41] and identified as interactor of β1 and β3 in our proximity screen (Fig. 1,3). Unfortunately, we were unable to successfully reduce Tensin3 expression by using siRNAs/shRNAs, or CRISPR/Cas9-mediated gene disruption in GE11 cells. As an alternative approach to investigate whether Tensin3 mediates the integrin-PEAK1 association, we generated PEAK1-deficient GE11/β1-BirA* cells using CRISPR/Cas9 and subsequently introduced wild-type or mutant forms of PEAK1 that carried a Y635F or Y1188F substitution.

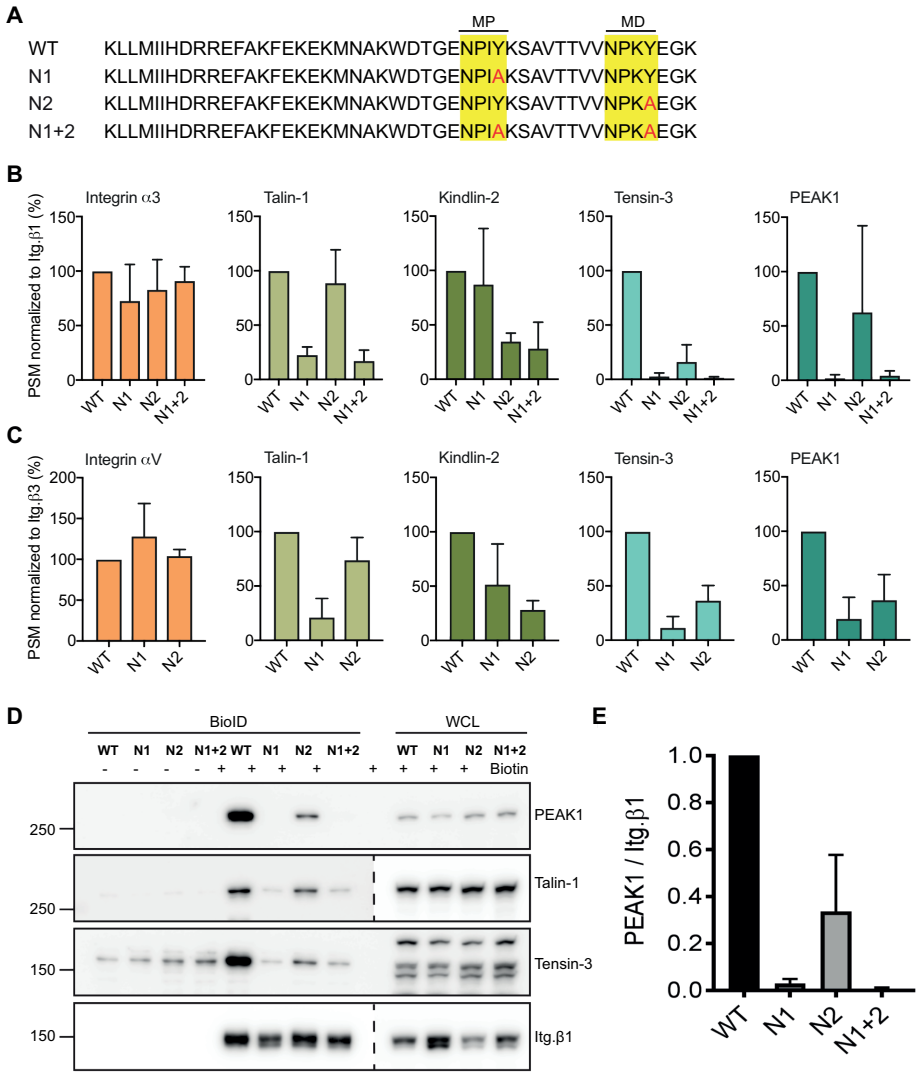

Fig. 3. Integrin β1 and β3 MP-NPxY motif required for interaction with PEAK1. (A) Amino acid sequence of integrin β1 cytoplasmic domain and β1 mutants that contain Y>A mutations in the membrane proximal (MP) and/or distal (MD) NPxY motifs. **(B,C)** PSM values of selected proximity interactors of β1 **(B)** and β3 **(C)** wild-type and NPxY/NxxY mutants as analyzed by mass spectrometry. PSM values are normalized to the PSM values of the integrin-BirA* fusion protein (n=3; bars show mean with s.d.). **(D)** Validation by Western blot of the experiments shown in **(B,C)**. **(E)**. Quantifications of PEAK1 signal intensities normalized to integrin β1 levels are shown (n=3; bars show mean with s.d.).

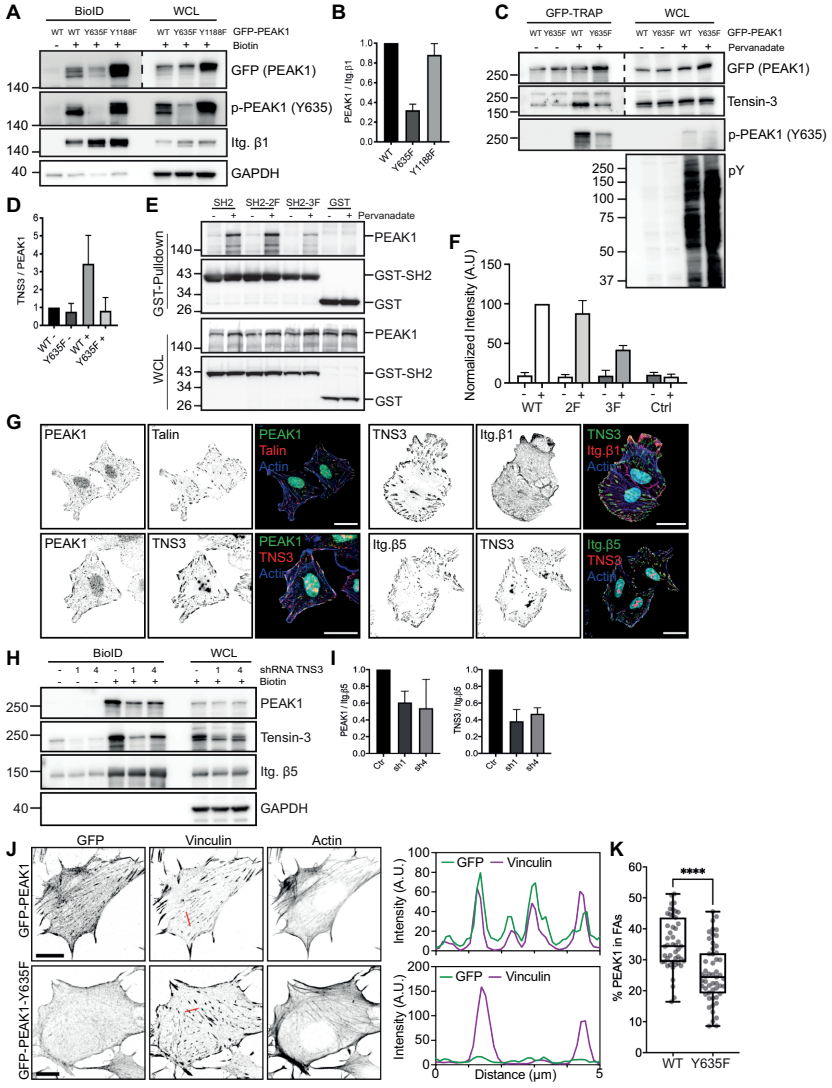

Fig. 4. Tensin3 binds to p-Y635 PEAK1. (A) Integrin β1-BirA* and GFP-PEAK1 wild-type or Y635F/Y1188F mutants were expressed in PEAK1-deficient GE11 cells. Representative Western blots of BioID assays are shown. **(B)** Quantifications of PEAK1 signal intensities normalized to integrin β1 levels are shown (n=3; bars show mean with s.d.). **(C)** GFP-PEAK1 wild-type and Y635F mutant were expressed in PEAK1-deficient SW480 cells. Cells were serum starved overnight and then treated with pervanadate for 10 min before cell lysis. Representative Western blots are shown of GFP-TRAP experiments. **(D)** Quantification of Tensin3 signal intensities normalized to PEAK1 (GFP) levels are shown (n=3; bars show mean with s.d.). **(E)** COS-7 cells transiently transfected with GST and GST-SH2 constructs together with a plasmid expressing HA-tagged full-length PEAK1 were treated with or without pervanadate for 10 min. Cell lysates derived from these transfected cells were subjected to a GST pull-down assay with glutathione-Sepharose (GE Healthcare). Whole cell

lysates (WCLs) and the pulled-down proteins were analyzed by Western blotting with antibodies against PEAK1 (D4G6J) and GST (2F3). **(F)** Quantification of Tensin3 signal intensities normalized to those of GST are shown (n=3; bars show mean with s.d.). **(G)** Colocalization of PEAK1, Talin, Tensin3, integrin β1 and β5 (shown in green or red in merge) in U251MG cells seeded on glass coverslips and cultured in medium supplemented with 10% FCS. Actin cytoskeleton (blue) and nuclei (cyan) are visualized. Scale bar, 20 µm. **(H)** Representative western blots of BioID assays performed using integrin β5-deficient U251MG cells expressing β5-BirA*, in which Tensin3 was depleted by two different shRNAs (1 and 4). Cells were treated with 50 µM biotin 24h before cell lysis. Quantifications of PEAK1 and Tensin3 signal intensities normalized to integrin β5 levels are shown (n=3; bars show mean with s.d.) in **(I)**. **(J)** Colocalization of vinculin and GFP-PEAK1 wild-type versus Y635F in PEAK1-deficient GE11 tet-ON integrin β1 cells treated with 1 µg/ml doxycycline for 48h to induce β1 expression. Scale bar, 10 µm. Quantifications of colocalization of FAs and PEAK1 (calculated as a percentage of total PEAK1) of immunofluorescence images as shown in **(K)**. FAs were stained with vinculin or pY. n=3, total number of cells analysed: 47 (WT); 53 (Y635F). Box plots range from the 25th to 75th percentile; central line indicates the median; whiskers show smallest to largest value. Mann-Whitney U test was performed to determine statistical significance. ****, P < 0.0001.

The Y635F mutation was selected based on the remarkable similarity of the ^{635}YDNL sequence in PEAK1 to the YDNV sequence present in Deleted in Liver Cancer 1 (DLC1), which mediates an interaction with the Tensin SH2 domain that precedes the PTB domain [42, 43]. Moreover, YDNL was identified as a binding peptide motif in a pY peptide library screen using the SH2 domain of Tensin [44]. On the other hand, Y1188 was shown to bind Shc1, which could represent an alternative connection between PEAK1 and the integrin β NPxY motif [25, 45-47]. BioID experiments combined with Western blot analysis clearly indicate that phosphorylation of Y635 in PEAK1 establishes the proximity interaction with integrin β1, while Shc1 binding is not required for the PEAK1-β1 interaction (Fig. 4A,B).

PEAK1 binds to Tensin3 in a phosphorylation-dependent manner to connect to integrins

To demonstrate that PEAK1 interacts directly with Tensin3 in a phosphorylation-specific manner, we expressed GFP-tagged PEAK1 or PEAK1-Y635F in CRISPR/Cas9-generated PEAK1-knockout human colorectal SW480 cells (Fig. S2A). GFP-PEAK1 was expressed at high levels and used for GFP pull down experiments. Cells were serum-starved overnight and treated with pervanadate, an irreversible inhibitor of protein tyrosine phosphatases, before lysis. GFP pull-down experiments show that Tensin3 is associated with PEAK1 in pervanadate-treated samples but hardly associated with PEAK1 in serum-starved PEAK1-WT or PEAK1-Y635F expressing cells (Fig. 4C,D). Furthermore, PEAK1-Y635F showed reduced co-localization with Tensin3 compared to PEAK1-WT (Fig. S2B). Intriguingly, the interaction between DLC1 and the SH2 domain of Tensin3/c-ten does not require phosphorylation of the YDNV motif in DLC1 [43, 48], and is less de-

pendent on the tyrosine phosphorylation of the Tensin3 SH2 domain [49]. This indicates that direct competition between DLC1 and PEAK1 for Tensin3 binding is unlikely because phosphorylation events upon growth factor stimulation would promote a switch from Tensin3-DLC1 to Tensin3-PEAK1 binding [50, 51].

PEAK1 is recruited to FAs upon phosphorylation by SFKs [23, 24, 30, 33]. In GE11 cells, where Src is already maximally active in the absence of EGF stimulation (i.e. its activity cannot be further increased by EGF stimulation, Fig. S2C), PEAK1 is highly phosphorylated on Y635 (Fig. S2D). To analyze if PEAK1 phosphorylation by Src is required for the PEAK1-Tensin3-β1 interaction, we conducted BioID assay using GE11/β1-BirA* cells treated with Saracatinib, an inhibitor of Src and Abl family kinases. Saracatinib treatment decreased tyrosine phosphorylation of PEAK1 and decreased the proximity interaction between PEAK1 and β1 (Fig. S2E), in line with previous findings [24]. GFP pull-down experiments using PEAK1-deficient GE11 cells expressing GFP-PEAK1 treated with Saracatinib confirmed that phosphorylation of PEAK1-Y635 is decreased upon Src inhibition (Fig. S2F).

Noticeably, Src has also been implicated in the phosphorylation of the SH2 domain of Tensin3 and tyrosine phosphorylation of the SH2 domain contributes to complex formation with several proteins [49]. To determine the importance of tyrosine phosphorylation of the SH2 domain for PEAK1 binding, we transiently expressed SH2 wild-type (SH2-WT), and SH2 double (SH2-2F; Y1206, Y1256F) and SH2 triple (SH2-3F; Y1173F, Y1206, Y1256F) mutants, engineered as GST fusion proteins together with PEAK1 in COS-7 cells. Cells were treated or untreated with pervanadate for 10 min. GST pull-down confirmed that the Tensin3 SH2-WT binds to PEAK1 and showed that tyrosine phosphorylation of the SH2 domain greatly enhanced the binding of Tensin3 to PEAK1 (Fig. 4E). Compared with Tensin3 SH2-WT, binding of the SH2-2F mutant to PEAK1 was only slightly reduced but that of the SH2-3F mutant by more than 50 % (Fig. 4E,F).

Next, we analyzed the PEAK1-Tensin3-integrin interaction in human U251MG glioblastoma cells, which express Tensin3 at high levels. PEAK1 and Tensin3 colocalized in FAs, as shown by immunofluorescence analysis (Fig. 4G). In line with our biochemistry results, PEAK1 was absent from cell-matrix adhesions in U251MG cells spread on fibronectin in the presence of the Src inhibitor Saracatinib (Fig. S2G). Integrin αVβ5 is the main RGD-binding integrin found to colocalize with Tensin3 and PEAK1 in FAs, while integrin β1 shows a more dispersed subcellular distribution and β3 could not be detected (Fig. 4G). We performed BioID assays by expressing β5-BirA* in β5-deficient U251MG cells that were additionally depleted of Tensin3 by shRNA-mediated gene knockdown. Depletion of Tensin3 by two different shRNAs reduced the PEAK1-integrin β5 proximity interaction (Fig. 4H,I), whilst the Talin1-integrin β5 interaction was not affected (Fig. S2H). Furthermore, PEAK1 was absent from cell-matrix adhesions in Tensin3-depleted cells (Fig. S2I). Finally, we compared the localization of GFP-PEAK1 wild-type versus Y635F in

FAs by immunofluorescence analysis. PEAK1-Y635F showed significantly reduced colocalization with the FA marker Vinculin compared to wild-type PEAK1 (Fig. 4J,K).
Taken together, these results indicate that Src-mediated phosphorylation of PEAK1 and the SH2 domain of Tensin3 promote their binding and facilitates PEAK1 interaction with the integrin β MP-NPxY motif.

Mapping the PEAK1 interactome

To identify additional proteins that interact with PEAK1, we employed a GFP-TRAP based affinity purification method combined with MS using PEAK1-deficient GE11 cells that express GFP-PEAK1, or the PEAK1-deficient cells as a negative control. This screen identified Shc1 and many proteins involved in the EGFR/Shc1 signaling network [25], including Asap1/2, Dab2ip, Grb2, Lrrk1, Ppp1ca/cc, Prag1, and Rasal2 as major PEAK1 interacting proteins (Fig. 5A). Both human and mouse PEAK1 are enriched in the GFP-PEAK1 sample, indicating that endogenous PEAK1 is not completely deleted in our GE11 control sample and dimerizes with the GFP-PEAK1 fusion protein [21]. Tensin3 was not found as a significant interactor of PEAK1 in this analysis (Fig. 5A). However, in a GFP-TRAP pull down assay using SW480 cells, a physical interaction between Tensin3 and PEAK1 could be demonstrated and was found to be dependent on the phosphorylation of PEAK1 at Y635 (Fig. 4C). Interestingly, Asap1/2 and Grb2 were recently identified as binding partners of the smaller PEAK family member PEAK3 [52], suggesting these proteins may interact with conserved domains in PEAK1-3.
Because PEAK1 is a scaffolding protein that functions in late EGFR-mediated signaling responses [25], we investigated whether the PEAK1 interactome changes upon 20 min EGF stimulation. The major interactors of PEAK1 remained unchanged after EGF treatment (Fig. S3), which is in line with our finding that Src is already maximally phosphorylated and PEAK1 phosphorylation is high in GE11 cells. However, Ptpn13 and Shroom2 were identified as additional, EGF-induced PEAK1-binding proteins (Fig. S6). The interaction of these proteins with PEAK1 likely depends on non-Src-mediated post-translational modifications that occur downstream of EGFR activation.
To further analyze the scaffolding function of PEAK1, we expressed different PEAK1 mutants in PEAK1-depleted GE11 cells and subsequently performed GFP pull-down experiments. Western blot analysis indicated that the Y1188F mutation almost completely abrogated the binding of PEAK1 to Shc1, but not to Rasal2 and only slightly to Grb2 (Fig. 5B). Grb2 binding to PEAK1-Y635E/F decreased by about 50%, whereas Shc1 was unchanged. Interestingly however, binding of tyrosine-phosphorylated Shc1 to PEAK1-Y635E/F was strongly decreased (Fig. 5B). In line with these biochemical findings, immunofluorescence analysis revealed that PEAK1 recruits Shc1 to FAs (Fig. 5C). Recruitment of Shc1 to FAs in PEAK1-deficient or PEAK1-Y1188F mutant cells shown by colocalization with phospho-paxillin is significantly reduced (Fig. 5C,D).

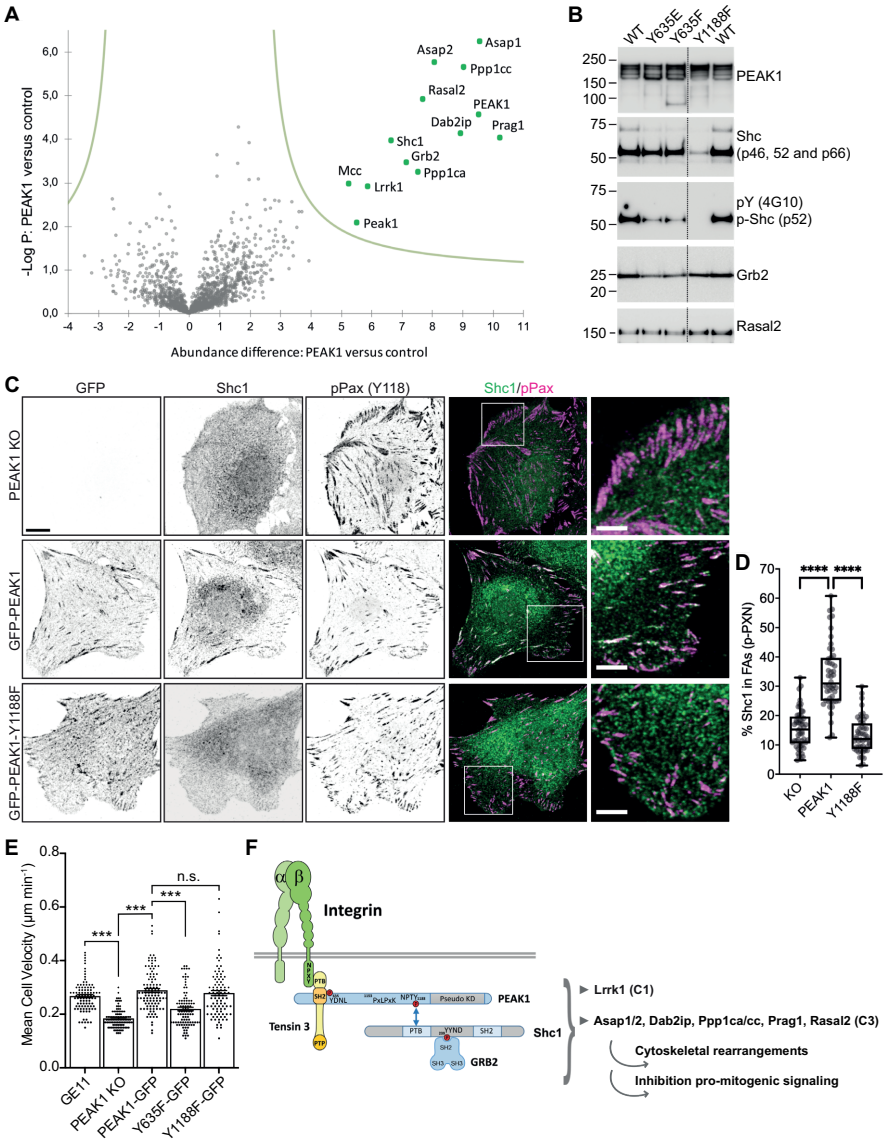

Fig. 5. PEAK1 recruits Shc1 to FAs. (A) GFP-PEAK1 was expressed in PEAK1-deficient GE11 cells to perform GFP-TRAP experiments followed by mass spectrometry analysis of binding partners. Volcano plot shows proteins enriched in PEAK1-GFP over control (PEAK1 knockout cells) samples. The logarithmic ratio of protein LFQs were plotted against negative logarithmic P values of a two-sided two samples t-test. The hyperbolic curve separates significantly enriched proteins (indicated in green) from common binders (FDR: 0.05, n=4). **(B)** GFP-PEAK1 wild-type or Y635E/Y635F/Y1188F mutants were expressed in PEAK1-deficient GE11 cells. Representative Western blots of GFP-TRAP experiments are shown. **(C)** Colocalization of GFP-PEAK1, Shc1 (green in merge),

and pPaxillin (magenta in merge) in PEAK1-deficient versus GFP-PEAK1 wild-type or Y1188F mutant- expressing GE11 cells. Scale bar, 10 µm; in magnified regions, 5 µm. **(D)** Quantifications of colocalization of Shc1 and phospho-Y118 Paxillin (calculated as a percentage of total Shc1) of immunofluorescence images as shown in **(C).** n=3, total number of cells analyzed: 52 (KO); 48 (PEAK1); 51 (Y1188F). Box plots range from the 25th to 75th percentile; central line indicates the median; whiskers show smallest to largest value. Mann-Whitney U test was performed to determine statistical significance. ****, P < 0.0001. **(E)** Migration of GE11 Tet-ON integrin β1 cells (wild type or PEAK1-deficient with or without rescue with the indicated PEAK1-GFP constructs) treated with 1 µg/ml doxycycline for 48h to induce β1 expression on fibronectin-coated plastic was analyzed in overnight movies. Kruskal-Wallis with Dunn's multiple comparisons test was performed to determine statistical significance; error bars show s.e.m., *** indicates p<0.0001; n = 93 (GE11), 105 (PEAK1 KO), 105 (PEAK1-GFP), 94 (PEAK1-Y635F), 94 (PEAK1-Y1188F) cells. **(F)** Model of PEAK1 and its binding partners. PEAK1 is connected to integrins by Tensin3, which binds to phospho-Y635 PEAK1 and the integrin β MP-NPxY motif. Shc1 binds phospho-Y1188 PEAK1. PEAK1 also interacts with proteins that were classified in different clusters based on their association rates with Shc1 upon EGF stimulation (Zheng *et al.* Nature. 2013), including the "cluster 1" (C1) proteins Grb2 and Lrrk1 and "cluster 3" (C3) proteins Asap1/2, Dab2ip, Ppp1ca/cc, Prag1, and Rasal2.

Because PEAK1-Y635F cannot bind Tensin3, we speculate that the phosphorylation of Shc1 is increased upon its recruitment to FAs, via PEAK1–Tensin3-integrin binding. Grb2, which also binds PEAK1-Y635, is not found in FAs and, therefore, does not play a major role in the localization and phosphorylation of Shc1 in FAs.

In line with our findings, Shc1 interacts with the FA-forming integrins, including α5β1 and αVβ3, and is phosphorylated by integrin β1 crosslinking or when cells are plated on fibronectin/vitronectin [53]. Shc1 controls various cellular processes in association with integrins and growth factor stimulation, including cell survival, proliferation, and migration [53, 54]. Therefore, we tested the contribution of PEAK1 phosphorylation at either Y635 or Y1188 to cell motility. GE11 cells depleted of endogenous PEAK1 migrated ~40% slower compared to WT GE11 cells; re-expression of PEAK1-GFP was able to rescue this reduction in cell velocity (Fig. 5E). The motility defect of the PEAK1-depleted GE11 cells was also rescued by expression of PEAK1-Y1188F-GFP, but not PEAK1-Y635F-GFP (Fig. 5E).

CONCLUSIONS

We report here that Tensin3 mediates the proximity interaction between PEAK1 and RGD-binding integrins through binding of its SH2 domain to PEAK1. Our findings indicate that PEAK1 mainly interacts with Shc1 and its associated protein cluster [25] and recruits Shc1 to FAs by interacting with Tensin3 and RGD-binding integrins (Fig. 5F). Moreover, integrins and growth factor receptors synergize to regulate cellular functions, including cell motility [55, 56]. In line with these findings, expression of PEAK1-Y635F, which showed

decreased binding to tyrosine-phosphorylated Shc1, was unable to restore the migration velocity of GE11 PEAK1 KO cells, unlike expression of PEAK1 wild-type (Fig. 5E). PEAK1 could be an important player in regulating integrin-growth factor receptor synergism, as it connects RGD-binding integrins to the protein cluster regulating late EGFR/Shc1 signaling [25].

MATERIALS AND METHODS

Antibodies

Primary antibodies used are listed in Supplementary Table 6. Secondary antibodies were as follows: goat anti-rabbit Alexa Fluor 488, goat anti-mouse Alexa Fluor 488, goat anti-mouse Texas Red, goat anti-mouse Alexa Fluor 568, donkey anti-rabbit Alexa Fluor 594, goat anti-rabbit Alexa Fluor 647, and goat anti-mouse Alexa Fluor 647 (Invitrogen), PE-conjugated donkey anti-rabbit antibody (BioLegend #406421), stabilized goat anti-mouse HRP-conjugated and stabilized goat anti-rabbit HRP-conjugated (Pierce; BioRad).

Generation of phospho-site-specific-Y365 PEAK1 antibodies

The phospho-peptide KVPIVINPNAY(PO3H2)DNLAIYKS with a cysteine added at the carboxyl-terminus was synthesized. The phospho-peptide was chemically conjugated with mariculture Keyhole Limpet Hemocyanin (mcKLH) using Imject™ Maleimide-Activated mcKLH Spin Kit (Thermo Fisher, 77666) according to the manufacturer's protocol. Briefly, 1 mg phospho-peptide dissolved in 500 µL conjugation buffer was mixed with 2 mg mcKLH dissolved in water for 2 hr at room temperature, the conjugate was desalted and collected by passing through the Zeba™ Spin Desalting Column. Two rabbits were immunized with 500 µg mcKLH-conjugated peptide in TiterMax® Gold-Adjuvant (Sigma Aldrich, T2684) and subsequently boosted with the same mcKLH conjugated phospho-peptide in Freund's incomplete adjuvant (Sigma Aldrich, F5506) at 4, 8 and 12 weeks. After the final immunization, blood of the animals was collected and IgG was purified on a Protein A Sepharose column (Pharmacia LKB Biotechnology Inc.). The phospho-specific antibodies were then purified by positive and negative affinity purification. For positive affinity purification, the phosphorylated peptide was covalently coupled to SulfoLink Coupling Gels from Pierce according to the manufacturer's protocol. Bound antibodies were eluted with 1M glycine-HCl, pH 2.9 and neutralized with an equal volume of 1 M Tris-HCl pH 8.5. Protein-containing fractions were pooled and concentrated with Amicon® Ultra-4 10K centrifugal filter devices (Millipore). After washing with PBS using the same filter devices, the concentrated protein fraction was added to a second column in which the corresponding non-phosphorylated peptide was covalently bound. All flow-through fractions containing antibodies were collected and stored at 4 °C.

Cell lines

GE11 β1 null cells were isolated from β1 chimeric embryos, as previously described [34]. SW480 and U251MG cell lines were obtained from the American Type Culture Collection. COS-7 cells have been described previously [57]. All cell lines were cultured in Dulbecco's modified Eagle's medium (DMEM) containing 10% heat-inactivated fetal bovine serum (FBS) and antibiotics. All cells were cultured at 37°C in a humidified, 5% CO_2 atmosphere.

Generation of PEAK1-deficient cells

The target sgRNA against mouse *Peak1* (exon 4; 5'-AAGCAATTCTTGCATTCGC-CAGG-3') or human *PEAK1* (exon 4; TGCCCGTGTTCCTGATGCGG-3') was cloned into pX330-U6-Chimeric_BB-CBh-hSpCas9 (a kind gift from Feng Zhang [58]; Addgene plasmid #42230). GE11 cells were transfected with this vector in combination with a blasticidin cassette, as previously described [59], and selected with 4 μg ml^{-1} blasticidin (Sigma) for four days following transfection. Transfected SW480 cells were selected with 2.5 μg ml^{-1} puromycin for 3 days.

Stable cellular transduction

The integrin β1 (mutants), generated as previously described [60], were subcloned into the *EcoR*I and *BamH*I sites of the pcDNA3.1 MCS-BirA(R118G)-HA vector [a gift from Kyle Roux (Addgene plasmid # 36047) [14]]. The integrin α3-BirA* construct was cloned by a 3-point ligation of a N-terminal PCR fragment containing an *EcoR*I site and a C-terminal part of 2.3 kb into *EcoR*I and *BamH*I sites of the pcDNA3.1 MCS-BirA(R118G)-HA vector. The integrin α5-BirA* construct was cloned by a 3-point ligation of a N-terminal part of 2.7 kb and a C-terminal PCR fragment lacking the stop codon into the *BamH*I site of the pcDNA3.1 MCS-BirA(R118G)-HA vector. The integrin α6-BirA* construct was described previously [19]. The integrin β1-BirA* (mutants), α5-BirA*, α3-BirA* and α6-BirA* constructs were cloned into the *SnaB*I site of the LZRS-IRES-Zeo vector.

The pRetroX-DSRed-SGK269 plasmid encoding human PEAK1 cDNA was kindly provided by Dr. Ling Liu. The PEAK1 construct was subcloned by a 3-point ligation of a N-terminal part of 4.9 kb and a C-terminal PCR fragment creating a stop codon and *Not*I site into *EcoR*I and *Not*I sites of pUC19 vector. Point mutants of PEAK1 Y635E, Y635F and Y1188F were generated by site-directed mutagenesis with the PCR-based overlap extension method using Pfu DNA polymerase (Promega) and were subcloned into the *EcoR*I and *Not*I sites of the pLZRS-EGFP vector, as previously described [61].
Retroviral vectors were introduced into Phoenix packaging cells using the Calcium Phosphate method. Virus-containing supernatant was collected 48h later. After retroviral transduction, infected cells were selected with 0.2 mg ml^{-1} zeocin (Invitrogen).

Generation of stable knockdown cell lines

Short hairpins against human Tensin3 (cloned into pLKO.1) were obtained from the MISSION® TRC shRNA collection and transfected into HEK 293FT cells using lipofectamine 2000 (Invitrogen). U251MG β5-BirA* expressing cells were generated as previously described [17], infected with the produced recombinant lentivirus, and selected with puromycin for 3 days. Target sequences included: CCGGACGCATAGGAGTGGTCATATCCTCGAGGATATGACCACTCCTATGCGTTTTTTG (shRNA 1) and CCGGCTCCCAGCAAAGCGTTCAAACCTCGAGGTTTGAACGCTTTGCTGGGAGTTTTTG (shRNA 4).

Transient transfection

Talin1 (M-040902-01-0020), Talin2 (M-065877-01-0020), Filamin-A (M-058520-02-0020), and Filamin-C (M-055631-01-0020) siGENOME SMARTpool siRNAs were purchased from Dharmacon. GE11 cells were transiently transfected using lipofectamine® 2000 (Invitrogen). Lipofectamine (20 µl ml^{-1}) and siRNA (0.5 µM) solutions in Opti-MEM were mixed (1:1) and incubated for 30 min at room temperature. Cells were incubated with the transfection solution overnight.

Flow cytometry

Cells were treated as indicated, trypsinized, and washed twice in PBS containing 2% FCS, followed by primary antibody (1:200 dilution) incubation for 1 h at 4°C. Then, cells were washed 3 times in PBS containing 2% FCS and incubated with secondary PE-conjugated antibodies (1:200 dilution) for 1 h at 4°C. After subsequent washing steps, desired cell populations were isolated by FACS sort using a Becton Dickinson FACSAria IIu or Beckman Coulter Moflo Astrios cell sorter.

BioID assay

Cells stably expressing the integrin subunit-BirA* fusion proteins were grown on 100 mm or 3 x 145 mm plates (for Western blot or mass spectrometry, respectively). Plates were coated with a laminin-332-rich matrix obtained by growing RAC-11P cells [62] to complete confluence, after which the plates were washed with PBS and incubated with 20 mM EDTA in PBS overnight at 4 °C. The RAC-11P cells were then removed by extensive washing with PBS.

Cells were washed in cold PBS, lysed in RIPA buffer (20 mM Tris-HCl (pH 7.5), 100 mM NaCl, 4 mM EDTA (pH 7.5), 1% NP-40, 0.1% SDS, 0.5% sodium deoxycholate) supplemented with a protease inhibitor cocktail (Sigma), and cleared by centrifugation at 14.000 x *g* for 30 min at 4°C. Lysates were incubated with Streptavidin Sepharose High Performance beads (GE Healthcare) overnight at 4°C. Beads were washes three times with NP40 buffer (20 mM Tris-HCl (pH 7.5), 100 mM NaCl, 4 mM EDTA (pH 7.5), 1% NP-40) and twice with PBS and the isolated biotinylated proteins were analyzed by mass spectrometry or Western blotting.

GFP pull down assays

Cells were washed in cold PBS, lysed in NP40 lysis buffer (20 mM Tris-HCl (pH 7.5), 100 mM NaCl, 4 mM EDTA (pH 7.5), 1% Nonidet P-40) supplemented with a protease inhibitor cocktail (Sigma) and 1.5 mM Na_3VO_4, 15 mM NaF (Cell Signaling Technology), and cleared by centrifugation at 14.000 x *g* for 30 min at 4°C. Lysates were incubated with GFP-Trap Agarose (Chromotek) according to manufacturer's instructions. Beads were washes three times with NP40 lysis buffer and twice with PBS and the isolated proteins were analyzed by mass spectrometry or Western blotting.

GST pull-down assay and Western blotting

COS-7 cells were co-transfected with plasmids expressing GST and GST fusion proteins of Tensin3 wild-type (SH2-WT) and SH2-domain mutants (SH2-2F; Y1206F/Y1256F) and (SH2-3F; Y173F/Y1206F/Y1256) [a kind gift from Douglas Lowy [49]], and a PEAK1 expressing plasmid using the DEAE-Dextran method [57]. Two days after transfection, the cells were treated with or without pervanadate and lysed in NP40 lysis buffer. After clearance of the lysates by centrifugation, equal amounts of proteins were used for pull-down assays by adding 25 µl glutathione Sepharose 4B beads (GE- Healthcare) and rotating for 4 hr at 4 °C. The beads were washed three time with NP40 lysis buffer and two times with PBS and bound proteins were then eluted with Laemmli sample buffer containing 2% β-mercaptoethanol at 95°C for 5 min. Proteins were separated by electrophoresis using Bolt Novex 4–12% gradient Bis-Tris gels (Invitrogen), transferred to Immobilon-P transfer membranes (Millipore Corp) and blocked for at least 30 min in 2% BSA in TBST buffer (10 mM Tris (pH 7.5), 150 mM NaCl, and 0.3% Tween-20). Primary antibody (diluted 1:1000 in 2% BSA in TBST buffer) incubation took place overnight at 4°C. After washing twice with TBST and twice with TBS buffer, blots were incubated for 1 h hour at room temperature with horseradish peroxidase–conjugated goat anti-mouse IgG or goat anti-rabbit IgG (diluted 1:3000 in 2% BSA in TBST buffer). After subsequent washing steps, the bound antibodies were detected by enhanced chemiluminescence using SuperSignal™ West Dura Extended Duration Substrate (ThermoFisher) or Clarity™ Western ECL Substrate (Bio-Rad) as described by the manufacturer. Signal intensities were quantified using ImageJ.

Mass spectrometry

For BioID experiments, Peptide mixtures were prepared, measured and analyzed as previously described [18], with the following exceptions. Peptide mixtures (33% of total digest) were loaded directly on the analytical column and analyzed by nanoLC-MS/MS on an Orbitrap Fusion Tribrid mass spectrometer equipped with a Proxeon nLC1200 system (Thermo Scientific). Solvent A was 0.1% formic acid/water and solvent B was 0.1% formic acid/80% acetonitrile. Peptides were eluted from the analytical column at a

constant flow of 250 nl/min in a 115-min gradient, containing a 100-min linear increase from 5% to 24% solvent B, followed by a 15-min wash at 90% solvent B.
Raw data were analyzed by MaxQuant (version 2.0.1.0) [63] using standard settings for label-free quantitation (LFQ). MS/MS data were searched against the Mus Musculus Swissprot database (17,082 entries, release 2021_07) complemented with a list of common contaminants and concatenated with the reversed version of all sequences. LFQ intensities were Log2-transformed in Perseus (version 1.6.15.0) [64], after which proteins were filtered for at least three valid values (out of 4 total). Differentially expressed proteins were determined using a Student's t-test (threshold: FDR: 5% and S0: 0.1).
GFP pull-down samples were loaded on an SDS-PAGE gel. Gel bands were excised into about 1x1 mm pieces and subjected to destaining and reduction alkylation of cysteines followed by overnight digestion with Trypsin (Promega). After digestion the peptides were desalted and concentrated via StageTips. Peptides were separated on a 40 min gradient on a 15 cm analytical column (75 µm inner diameter) packed with 1.9 µm ReproSil Gold C18 reversed phase particles (Dr. Maisch, Tübingen, Germany). The column was maintained at 50°C and peptides were directly sprayed into a Q Exactive HF mass spectrometer via a nano-electrospray ionization source. The mass spectrometer was operated on a data dependent mode with up to top15 precursors were selected for fragmentation. Raw data were processed using MaxQuant (version 1.6.0.15) and all identifications were filtered at 1% false discovery rates.

Immunofluorescence

Subconfluent cells were fixed with 2% paraformaldehyde for 10 min, permeabilized with 0.2% Triton-X-100 for 5 min, and blocked with PBS containing 2% BSA (Sigma) for at least 30 min. Next, cells were incubated with the primary antibodies for 1 h at room temperature. Cells were washed three times before incubation with the secondary antibodies for 1 h. Additionally, the nuclei were stained with DAPI and filamentous actin was visualized using Alexa Fluor 488 or 647-conjugated phalloidin (Biolegend; AAT Bioquest). After three washing steps with PBS, the coverslips were mounted onto glass slides in Mowiol. Images were obtained at room temperature using a Leica TCS SP5 confocal microscope with a AOBS scan head (Leica, 158001107), controlled using Leica LAS AF SP5 software (ver. 2.7.4), with a 63x/1.4 Oil CS HC PL APO objective (Leica, 11506350), with filter cubes for 488/eGFP (Leica, 15525302), 568/mCherry (Leica, 15525303), DAPI (Leica, 15525301).

Cell motility

GE11 Tet-ON integrin β1 cells (WT, PEAK1 KO, PEAK1 KO stably expressing PEAK1-GFP, PEAK1-Y635F-GFP or PEAK1-Y1188F-GFP) were cultured for at least 48 hrs with 1 µg/ml doxycycline to induce β1 integrin expression, then plated onto fibronectin-coated (10

µg/ml in PBS) plastic 12-well plates (20,000 cells per well) in DMEM containing 0.5% FBS, antibiotics, and doxycycline (1 µg/ml). After culture overnight, the medium was exchanged for DMEM containing 0.5% FBS, antibiotics, and doxycycline (1 µg/ml), and cells were transferred to the heated stage (37°C with 5% CO_2) of a Zeiss AxioObserver Z.1 microscope. Phase-contrast images were acquired with a 10x/0.30 EC Plan-Neofluar Ph1 objective (Zeiss), captured with a Zeiss AxioCam MRm. Images were acquired every 10 minutes for 20 hours. Cells were tracked manually using ImageJ; tracking data was analysed using the Chemotaxis Tool plugin (Ibidi).

Image analysis and statistical analysis

Image analysis was performed using Fiji (ImageJ) [65, 66]. To quantify Shc1 clustering in FAs (based on Paxillin staining), background was subtracted in both channels using a bilateral filter and the ROI was selected at the cell periphery. Colocalization of Shc1 and FAs was determined using the Image Calculator (command "multiply") on both channels and calculating the area of overlapping fraction as a percentage of the total Shc1 area per cell using the Analyze Particle function. The amount of GFP-PEAK1 (WT or Y635F) present in FAs was calculated in the same manner, using vinculin staining as a marker for FAs.

Mann-Whitney test (two-tailed P value) was performed using GraphPad Prism (version 7.0c). In figures, statistically significant values are shown as ****, $P < 0.0001$. Graphs were made in GraphPad Prism and show all data points. Data distribution was assumed to be normal but this was not formally tested.

ACKNOWLEDGEMENTS

We thank Anne Cress, David Critchley, Roger Daly, Marina Glukhova, Simon Goodman, Douglas Lowy, Jacques Neefjes, Ellen van der Schoot, and NKI colleagues for sharing cells and reagents.

This work was supported by the Dutch Cancer Society (project 12143). Liesbeth Hoekman and Onno B. Bleijerveld are supported by the Dutch NWO X-omics Initiative. A. Sonnenberg and R. Fässler would like to thank the Alexander von Humboldt Foundation for supporting A. Sonnenberg during his sabbatical year at the Max Planck Institute.

REFERENCES

1. Hynes, R.O., *Integrins: bidirectional, allosteric signaling machines.* Cell, 2002. **110**(6): p. 673-87.
2. Geiger, B. and K.M. Yamada, *Molecular architecture and function of matrix adhesions.* Cold Spring Harb Perspect Biol, 2011. **3**(5).
3. Morse, E.M., N.N. Brahme, and D.A. Calderwood, *Integrin cytoplasmic tail interactions.* Biochemistry, 2014. **53**(5): p. 810-20.
4. Winograd-Katz, S.E., R. Fassler, B. Geiger, and K.R. Legate, *The integrin adhesome: from genes and proteins to human disease.* Nat Rev Mol Cell Biol, 2014. **15**(4): p. 273-88.
5. Horton, E.R., J.D. Humphries, J. James, M.C. Jones, J.A. Askari, and M.J. Humphries, *The integrin adhesome network at a glance.* J Cell Sci, 2016. **129**(22): p. 4159-4163.
6. Manninen, A. and M. Varjosalo, *A proteomics view on integrin-mediated adhesions.* Proteomics, 2017. **17**(3-4).
7. Zaidel-Bar, R., S. Itzkovitz, A. Ma'ayan, R. Iyengar, and B. Geiger, *Functional atlas of the integrin adhesome.* Nat Cell Biol, 2007. **9**(8): p. 858-67.
8. Schiller, H.B., C.C. Friedel, C. Boulegue, and R. Fassler, *Quantitative proteomics of the integrin adhesome show a myosin II-dependent recruitment of LIM domain proteins.* EMBO Rep, 2011. **12**(3): p. 259-66.
9. Schiller, H.B., M.R. Hermann, J. Polleux, T. Vignaud, S. Zanivan, C.C. Friedel, Z. Sun, A. Raducanu, K.E. Gottschalk, M. Thery, M. Mann, and R. Fassler, *beta1- and alphav-class integrins cooperate to regulate myosin II during rigidity sensing of fibronectin-based microenvironments.* Nat Cell Biol, 2013. **15**(6): p. 625-36.
10. Robertson, J., G. Jacquemet, A. Byron, M.C. Jones, S. Warwood, J.N. Selley, D. Knight, J.D. Humphries, and M.J. Humphries, *Defining the phospho-adhesome through the phosphoproteomic analysis of integrin signalling.* Nat Commun, 2015. **6**: p. 6265.
11. Humphries, J.D., A. Byron, M.D. Bass, S.E. Craig, J.W. Pinney, D. Knight, and M.J. Humphries, *Proteomic analysis of integrin-associated complexes identifies RCC2 as a dual regulator of Rac1 and Arf6.* Sci Signal, 2009. **2**(87): p. ra51.
12. Ng, D.H., J.D. Humphries, A. Byron, A. Millon-Fremillon, and M.J. Humphries, *Microtubule-dependent modulation of adhesion complex composition.* PLoS One, 2014. **9**(12): p. e115213.
13. Horton, E.R., A. Byron, J.A. Askari, D.H.J. Ng, A. Millon-Fremillon, J. Robertson, E.J. Koper, N.R. Paul, S. Warwood, D. Knight, J.D. Humphries, and M.J. Humphries, *Definition of a consensus integrin adhesome and its dynamics during adhesion complex assembly and disassembly.* Nat Cell Biol, 2015. **17**(12): p. 1577-1587.
14. Roux, K.J., D.I. Kim, M. Raida, and B. Burke, *A promiscuous biotin ligase fusion protein identifies proximal and interacting proteins in mammalian cells.* J Cell Biol, 2012. **196**(6): p. 801-10.
15. Dong, J.M., F.P. Tay, H.L. Swa, J. Gunaratne, T. Leung, B. Burke, and E. Manser, *Proximity biotinylation provides insight into the molecular composition of focal adhesions at the nanometer scale.* Sci Signal, 2016. **9**(432): p. rs4.
16. Chastney, M.R., C. Lawless, J.D. Humphries, S. Warwood, M.C. Jones, D. Knight, C. Jorgensen, and M.J. Humphries, *Topological features of integrin adhesion complexes revealed by multiplexed proximity biotinylation.* J Cell Biol, 2020. **219**(8).

17. Zuidema, A., W. Wang, M. Kreft, L. Te Molder, L. Hoekman, O.B. Bleijerveld, L. Nahidiazar, H. Janssen, and A. Sonnenberg, *Mechanisms of integrin alphaVbeta5 clustering in flat clathrin lattices.* J Cell Sci, 2018. **131**(21).
18. Wang, W., A. Zuidema, L. Te Molder, L. Nahidiazar, L. Hoekman, T. Schmidt, S. Coppola, and A. Sonnenberg, *Hemidesmosomes modulate force generation via focal adhesions.* J Cell Biol, 2020. **219**(2).
19. Te Molder, L., L. Hoekman, M. Kreft, O. Bleijerveld, and A. Sonnenberg, *Comparative interactomics analysis reveals potential regulators of alpha6beta4 distribution in keratinocytes.* Biol Open, 2020. **9**(8).
20. Patel, O., M.D.W. Griffin, S. Panjikar, W. Dai, X. Ma, H. Chan, C. Zheng, A. Kropp, J.M. Murphy, R.J. Daly, and I.S. Lucet, *Structure of SgK223 pseudokinase reveals novel mechanisms of homotypic and heterotypic association.* Nat Commun, 2017. **8**(1): p. 1157.
21. Patel, O., M.J. Roy, J.M. Murphy, and I.S. Lucet, *The PEAK family of pseudokinases, their role in cell signalling and cancer.* FEBS J, 2020. **287**(19): p. 4183-4197.
22. Ha, B.H. and T.J. Boggon, *The crystal structure of pseudokinase PEAK1 (Sugen kinase 269) reveals an unusual catalytic cleft and a novel mode of kinase fold dimerization.* J Biol Chem, 2018. **293**(5): p. 1642-1650.
23. Wang, Y., J.A. Kelber, H.S. Tran Cao, G.T. Cantin, R. Lin, W. Wang, S. Kaushal, J.M. Bristow, T.S. Edgington, R.M. Hoffman, M. Bouvet, J.R. Yates, 3rd, and R.L. Klemke, *Pseudopodium-enriched atypical kinase 1 regulates the cytoskeleton and cancer progression [corrected].* Proc Natl Acad Sci U S A, 2010. **107**(24): p. 10920-5.
24. Bristow, J.M., T.A. Reno, M. Jo, S.L. Gonias, and R.L. Klemke, *Dynamic phosphorylation of tyrosine 665 in pseudopodium-enriched atypical kinase 1 (PEAK1) is essential for the regulation of cell migration and focal adhesion turnover.* J Biol Chem, 2013. **288**(1): p. 123-31.
25. Zheng, Y., C. Zhang, D.R. Croucher, M.A. Soliman, N. St-Denis, A. Pasculescu, L. Taylor, S.A. Tate, W.R. Hardy, K. Colwill, A.Y. Dai, R. Bagshaw, J.W. Dennis, A.C. Gingras, R.J. Daly, and T. Pawson, *Temporal regulation of EGF signalling networks by the scaffold protein Shc1.* Nature, 2013. **499**(7457): p. 166-71.
26. Ding, C., W. Tang, X. Fan, X. Wang, H. Wu, H. Xu, W. Xu, W. Gao, and G. Wu, *Overexpression of PEAK1 contributes to epithelial-mesenchymal transition and tumor metastasis in lung cancer through modulating ERK1/2 and JAK2 signaling.* Cell Death Dis, 2018. **9**(8): p. 802.
27. Kelber, J.A., T. Reno, S. Kaushal, C. Metildi, T. Wright, K. Stoletov, J.M. Weems, F.D. Park, E. Mose, Y. Wang, R.M. Hoffman, A.M. Lowy, M. Bouvet, and R.L. Klemke, *KRas induces a Src/PEAK1/ErbB2 kinase amplification loop that drives metastatic growth and therapy resistance in pancreatic cancer.* Cancer Res, 2012. **72**(10): p. 2554-64.
28. Fujimura, K., T. Wright, J. Strnadel, S. Kaushal, C. Metildi, A.M. Lowy, M. Bouvet, J.A. Kelber, and R.L. Klemke, *A hypusine-eIF5A-PEAK1 switch regulates the pathogenesis of pancreatic cancer.* Cancer Res, 2014. **74**(22): p. 6671-81.
29. Strnadel, J., S. Choi, K. Fujimura, H. Wang, W. Zhang, M. Wyse, T. Wright, E. Gross, C. Peinado, H.W. Park, J. Bui, J. Kelber, M. Bouvet, K.L. Guan, and R.L. Klemke, *eIF5A-PEAK1 Signaling Regulates YAP1/TAZ Protein Expression and Pancreatic Cancer Cell Growth.* Cancer Res, 2017. **77**(8): p. 1997-2007.

30. Croucher, D.R., F. Hochgrafe, L. Zhang, L. Liu, R.J. Lyons, D. Rickwood, C.M. Tactacan, B.C. Browne, N. Ali, H. Chan, R. Shearer, D. Gallego-Ortega, D.N. Saunders, A. Swarbrick, and R.J. Daly, *Involvement of Lyn and the atypical kinase SgK269/PEAK1 in a basal breast cancer signaling pathway.* Cancer Res, 2013. **73**(6): p. 1969-80.
31. Agajanian, M., A. Campeau, M. Hoover, A. Hou, D. Brambilla, S.L. Kim, R.L. Klemke, and J.A. Kelber, *PEAK1 Acts as a Molecular Switch to Regulate Context-Dependent TGFbeta Responses in Breast Cancer.* PLoS One, 2015. **10**(8): p. e0135748.
32. Abu-Thuraia, A., M.A. Goyette, J. Boulais, C. Delliaux, C. Apcher, C. Schott, R. Chidiac, H. Bagci, M.P. Thibault, D. Davidson, M. Ferron, A. Veillette, R.J. Daly, A.C. Gingras, J.P. Gratton, and J.F. Cote, *AXL confers cell migration and invasion by hijacking a PEAK1-regulated focal adhesion protein network.* Nat Commun, 2020. **11**(1): p. 3586.
33. Leroy, C., C. Fialin, A. Sirvent, V. Simon, S. Urbach, J. Poncet, B. Robert, P. Jouin, and S. Roche, *Quantitative phosphoproteomics reveals a cluster of tyrosine kinases that mediates SRC invasive activity in advanced colon carcinoma cells.* Cancer Res, 2009. **69**(6): p. 2279-86.
34. Gimond, C., A. van Der Flier, S. van Delft, C. Brakebusch, I. Kuikman, J.G. Collard, R. Fassler, and A. Sonnenberg, *Induction of cell scattering by expression of beta1 integrins in beta1-deficient epithelial cells requires activation of members of the rho family of GTPases and downregulation of cadherin and catenin function.* J Cell Biol, 1999. **147**(6): p. 1325-40.
35. Bouchet, B.P., R.E. Gough, Y.C. Ammon, D. van de Willige, H. Post, G. Jacquemet, A.M. Altelaar, A.J. Heck, B.T. Goult, and A. Akhmanova, *Talin-KANK1 interaction controls the recruitment of cortical microtubule stabilizing complexes to focal adhesions.* Elife, 2016. **5**.
36. Sun, Z., H.Y. Tseng, S. Tan, F. Senger, L. Kurzawa, D. Dedden, N. Mizuno, A.A. Wasik, M. Thery, A.R. Dunn, and R. Fassler, *Kank2 activates talin, reduces force transduction across integrins and induces central adhesion formation.* Nat Cell Biol, 2016. **18**(9): p. 941-53.
37. Charrin, S., S. Jouannet, C. Boucheix, and E. Rubinstein, *Tetraspanins at a glance.* J Cell Sci, 2014. **127**(Pt 17): p. 3641-8.
38. Calderwood, D.A., Y. Fujioka, J.M. de Pereda, B. Garcia-Alvarez, T. Nakamoto, B. Margolis, C.J. McGlade, R.C. Liddington, and M.H. Ginsberg, *Integrin beta cytoplasmic domain interactions with phosphotyrosine-binding domains: a structural prototype for diversity in integrin signaling.* Proc Natl Acad Sci U S A, 2003. **100**(5): p. 2272-7.
39. Moser, M., K.R. Legate, R. Zent, and R. Fassler, *The tail of integrins, talin, and kindlins.* Science, 2009. **324**(5929): p. 895-9.
40. Kiema, T., Y. Lad, P. Jiang, C.L. Oxley, M. Baldassarre, K.L. Wegener, I.D. Campbell, J. Ylanne, and D.A. Calderwood, *The molecular basis of filamin binding to integrins and competition with talin.* Mol Cell, 2006. **21**(3): p. 337-47.
41. McCleverty, C.J., D.C. Lin, and R.C. Liddington, *Structure of the PTB domain of Tensin1 and a model for its recruitment to fibrillar adhesions.* Protein Sci, 2007. **16**(6): p. 1223-9.
42. Yam, J.W., F.C. Ko, C.Y. Chan, D.Y. Jin, and I.O. Ng, *Interaction of deleted in liver cancer 1 with Tensin2 in caveolae and implications in tumor suppression.* Cancer Res, 2006. **66**(17): p. 8367-72.
43. Liao, Y.C., L. Si, R.W. deVere White, and S.H. Lo, *The phosphotyrosine-independent interaction of DLC-1 and the SH2 domain of cten regulates focal adhesion localization and growth suppression activity of DLC-1.* J Cell Biol, 2007. **176**(1): p. 43-9.

44. Wavreille, A.S. and D. Pei, *A chemical approach to the identification of Tensin-binding proteins.* ACS Chem Biol, 2007. **2**(2): p. 109-18.
45. Cowan, K.J., D.A. Law, and D.R. Phillips, *Identification of shc as the primary protein binding to the tyrosine-phosphorylated beta 3 subunit of alpha IIbbeta 3 during outside-in integrin platelet signaling.* J Biol Chem, 2000. **275**(46): p. 36423-9.
46. Deshmukh, L., V. Gorbatyuk, and O. Vinogradova, *Integrin {beta}3 phosphorylation dictates its complex with the Shc phosphotyrosine-binding (PTB) domain.* J Biol Chem, 2010. **285**(45): p. 34875-84.
47. Smith, M.J., W.R. Hardy, J.M. Murphy, N. Jones, and T. Pawson, *Screening for PTB domain binding partners and ligand specificity using proteome-derived NPXY peptide arrays.* Mol Cell Biol, 2006. **26**(22): p. 8461-74.
48. Cao, X., T. Kaneko, J.S. Li, A.D. Liu, C. Voss, and S.S. Li, *A phosphorylation switch controls the spatiotemporal activation of Rho GTPases in directional cell migration.* Nat Commun, 2015. **6**: p. 7721.
49. Qian, X., G. Li, W.C. Vass, A. Papageorge, R.C. Walker, L. Asnaghi, P.J. Steinbach, G. Tosato, K. Hunter, and D.R. Lowy, *The Tensin protein, including its SH2 domain, is phosphorylated by Src and contributes to tumorigenesis and metastasis.* Cancer Cell, 2009. **16**(3): p. 246-58.
50. Cui, Y., Y.C. Liao, and S.H. Lo, *Epidermal growth factor modulates tyrosine phosphorylation of a novel Tensin family member, Tensin3.* Mol Cancer Res, 2004. **2**(4): p. 225-32.
51. Chumbalkar, V., K. Latha, Y. Hwang, R. Maywald, L. Hawley, R. Sawaya, L. Diao, K. Baggerly, W.K. Cavenee, F.B. Furnari, and O. Bogler, *Analysis of phosphotyrosine signaling in glioblastoma identifies STAT5 as a novel downstream target of DeltaEGFR.* J Proteome Res, 2011. **10**(3): p. 1343-52.
52. Hou, J., E.V. Nguyen, M. Surudoi, M.J. Roy, O. Patel, I.S. Lucet, X. Ma, and R.J. Daly, *Distinct PEAK3 interactors and outputs expand the signaling potential of the PEAK pseudokinase family.* Sci Signal, 2022. **15**(722): p. eabj3554.
53. Wary, K.K., F. Mainiero, S.J. Isakoff, E.E. Marcantonio, and F.G. Giancotti, *The adaptor protein Shc couples a class of integrins to the control of cell cycle progression.* Cell, 1996. **87**(4): p. 733-43.
54. Mauro, L., D. Sisci, M. Bartucci, M. Salerno, J. Kim, T. Tam, M.A. Guvakova, S. Ando, and E. Surmacz, *SHC-alpha5beta1 integrin interactions regulate breast cancer cell adhesion and motility.* Exp Cell Res, 1999. **252**(2): p. 439-48.
55. Morello, V., S. Cabodi, S. Sigismund, M.P. Camacho-Leal, D. Repetto, M. Volante, M. Papotti, E. Turco, and P. Defilippi, *beta1 integrin controls EGFR signaling and tumorigenic properties of lung cancer cells.* Oncogene, 2011. **30**(39): p. 4087-96.
56. Miyamoto, S., H. Teramoto, J.S. Gutkind, and K.M. Yamada, *Integrins can collaborate with growth factors for phosphorylation of receptor tyrosine kinases and MAP kinase activation: roles of integrin aggregation and occupancy of receptors.* J Cell Biol, 1996. **135**(6 Pt 1): p. 1633-42.
57. De Melker, A.A., D. Kramer, I. Kuikman, and A. Sonnenberg, *The two phenylalanines in the GFFKR motif of the integrin alpha6A subunit are essential for heterodimerization.* Biochem J, 1997. **328 (Pt 2)**: p. 529-37.

58. Cong, L., F.A. Ran, D. Cox, S. Lin, R. Barretto, N. Habib, P.D. Hsu, X. Wu, W. Jiang, L.A. Marraffini, and F. Zhang, *Multiplex genome engineering using CRISPR/Cas systems.* Science, 2013. **339**(6121): p. 819-23.
59. Heijink, A.M., V.A. Blomen, X. Bisteau, F. Degener, F.Y. Matsushita, P. Kaldis, F. Foijer, and M.A. van Vugt, *A haploid genetic screen identifies the G1/S regulatory machinery as a determinant of Wee1 inhibitor sensitivity.* Proc Natl Acad Sci U S A, 2015. **112**(49): p. 15160-5.
60. Margadant, C., M. Kreft, D.J. de Groot, J.C. Norman, and A. Sonnenberg, *Distinct roles of talin and kindlin in regulating integrin alpha5beta1 function and trafficking.* Curr Biol, 2012. **22**(17): p. 1554-63.
61. Ketema, M., M. Kreft, P. Secades, H. Janssen, and A. Sonnenberg, *Nesprin-3 connects plectin and vimentin to the nuclear envelope of Sertoli cells but is not required for Sertoli cell function in spermatogenesis.* Mol Biol Cell, 2013. **24**(15): p. 2454-66.
62. Delwel, G.O., A.A. de Melker, F. Hogervorst, L.H. Jaspars, D.L. Fles, I. Kuikman, A. Lindblom, M. Paulsson, R. Timpl, and A. Sonnenberg, *Distinct and overlapping ligand specificities of the alpha 3A beta 1 and alpha 6A beta 1 integrins: recognition of laminin isoforms.* Mol Biol Cell, 1994. **5**(2): p. 203-15.
63. Cox, J., M.Y. Hein, C.A. Luber, I. Paron, N. Nagaraj, and M. Mann, *Accurate proteome-wide label-free quantification by delayed normalization and maximal peptide ratio extraction, termed MaxLFQ.* Mol Cell Proteomics, 2014. **13**(9): p. 2513-26.
64. Tyanova, S., T. Temu, P. Sinitcyn, A. Carlson, M.Y. Hein, T. Geiger, M. Mann, and J. Cox, *The Perseus computational platform for comprehensive analysis of (prote)omics data.* Nat Methods, 2016. **13**(9): p. 731-40.
65. Schindelin, J., I. Arganda-Carreras, E. Frise, V. Kaynig, M. Longair, T. Pietzsch, S. Preibisch, C. Rueden, S. Saalfeld, B. Schmid, J.Y. Tinevez, D.J. White, V. Hartenstein, K. Eliceiri, P. Tomancak, and A. Cardona, *Fiji: an open-source platform for biological-image analysis.* Nat Methods, 2012. **9**(7): p. 676-82.
66. Schneider, C.A., W.S. Rasband, and K.W. Eliceiri, *NIH Image to ImageJ: 25 years of image analysis.* Nat Methods, 2012. **9**(7): p. 671-5.

SUPPLEMENTARY FIGURES

A

Uniprot Accession	Gene Name	Description	Uniprot Accession	Gene Name	Description
P26039	Tln1	Talin-1	Q8CDJ8	Ston1	Stonin-1
P43406	Itgav	Integrin alpha-V	B9EJ80	Pdzd8	PDZ domain-containing protein 8
Q69ZN7	Myof	Myoferlin	Q61029	Tmpo	Lamina-associated polypeptide 2, isoforms β, δ, ε, γ
Q69Z38	Peak1	Pseudopodium-enriched atypical kinase 1	Q8BQZ4	Ralgapb	Ral GTPase-activating protein subunit beta
Q80UU9	Pgrmc2	Membrane-associated progesterone receptor component 2	P18572	Bsg	Basigin
Q91WL8	Wwox	WW domain-containing oxidoreductase	P32507	Pvrl2	Nectin-2
Q8K1S3	Unc5b	Netrin receptor UNC5B	Q9D0F3	Lman1	Protein ERGIC-53
O54890	Itgb3	Integrin beta-3	Q71LX4	Tln2	Talin-2
Q811D0	Dlg1	Disks large homolog 1	Q3UR85	Myrf	Myelin regulatory factor
F8VQB6	Myo10	Unconventional myosin-X	Q5DTU0	Afap1l2	Actin filament-associated protein 1-like 2
Q5SYH2	Tmem199	Transmembrane protein 199	Q03145	Epha2	Ephrin type-A receptor 2
O70318	Epb41l2	Band 4.1-like protein 2	Q9QY76	Vapb	Vesicle-associated membrane protein-associated protein B
Q99P72	Rtn4	Reticulon-4	O09044	Snap23	Synaptosomal-associated protein 23
Q9WTQ5	Akap12	A-kinase anchor protein 12	Q99KW3	Triobp	TRIO and F-actin-binding protein
Q8C1B7	Septin11	Septin-11	Q8CIN4	Pak2	Serine/threonine-protein kinase PAK 2
P70302	Stim1	Stromal interaction molecule 1	Q9Z0U1	Tjp2	Tight junction protein ZO-2
Q8BX02	Kank2	KN motif and ankyrin repeat domain-containing protein 2	Q9DBR4	Apbb2	Amyloid beta A4 precursor protein-binding family B member 2
Q62407	Speg	Striated muscle-specific serine/threonine-protein kinase	Q9WV55	Vapa	Vesicle-associated membrane protein-associated protein A
P56395	Cyb5a	Cytochrome b5	Q3UMF0	Cobll1	Cordon-bleu protein-like 1
Q6P9J9	Ano6	Anoctamin-6	Q9EPE9	Atp13a1	Manganese-transporting ATPase 13A1
Q9Z2B5	Eif2ak3	Eukaryotic translation initiation factor 2-alpha kinase 3	Q5SSZ5	Tns3	Tensin-3
P47740	Aldh3a2	Fatty aldehyde dehydrogenase	Q9WVC3	Cav2	Caveolin-2
O70252	Hmox2	Heme oxygenase 2	Q5FWI3	Tmem2	Transmembrane protein 2
Q8CIB5	Fermt2	Fermitin family homolog 2	Q6P1H6	Ankle2	Ankyrin repeat and LEM domain-containing protein 2

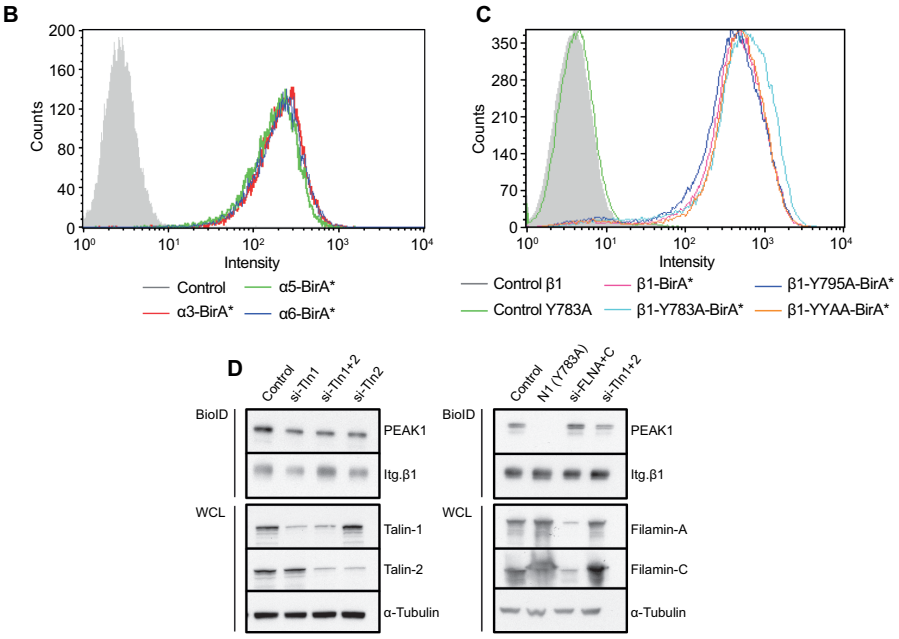

Fig. S1. Identification of overlapping proteins in β1- and β3-BioID data sets, expression of integrin subunits and knockdown of integrin NPxY- binding proteins. (A) Table of proteins identified in both the integrin β1-BirA* and integrin β3-BirA* BioID datasets. **(B, C)** Flow cytometry plots of integrin β1 in GE11 cells stably expressing the indicated integrin alpha **(B)** or beta **(C)** subunits with a C-terminal BirA* tag. **(D)** Western blots of BioID assays performed using GE11/β1-BirA* cells transfected with siRNAs against Talin1/2 or Filamin A/C 72h before cell lysis. All samples were treated with 50 μM biotin 24h before cell lysis.

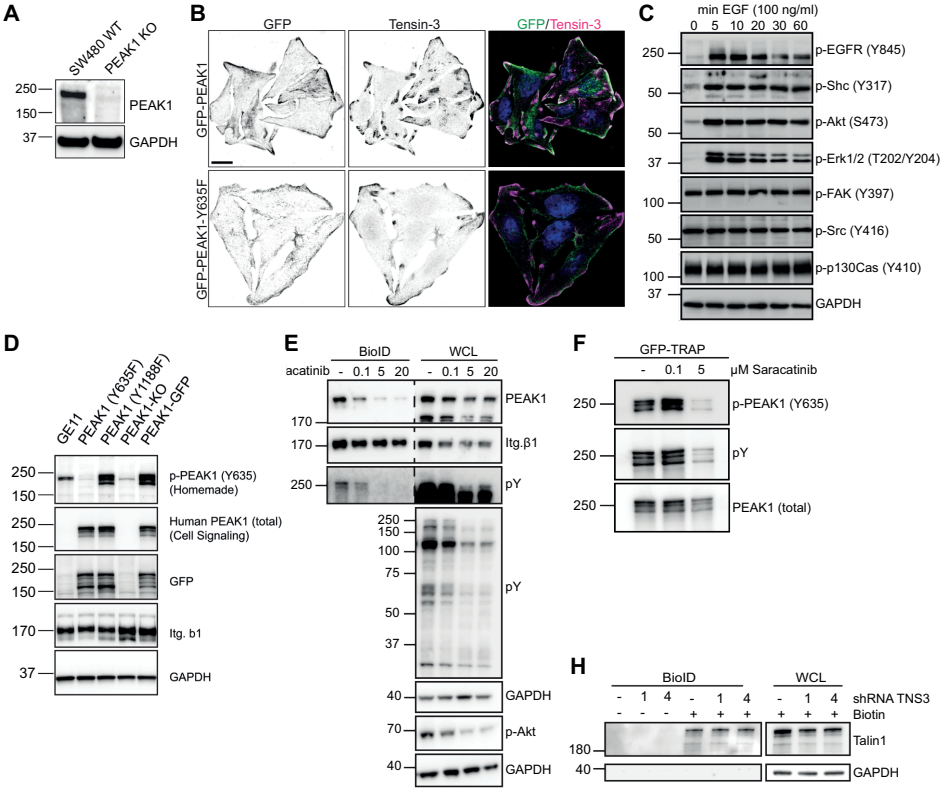
A
SW480 WT
PEAK1 KO
250
150
37
PEAK1
GAPDH
B
GFP
Tensin-3
GFP/Tensin-3
GFP-PEAK1
GFP-PEAK1-Y635F
C
min EGF (100 ng/ml)
0 5 10 20 30 60
250
50
50
37
100
50
100
37
p-EGFR (Y845)
p-Shc (Y317)
p-Akt (S473)
p-Erk1/2 (T202/Y204)
p-FAK (Y397)
p-Src (Y416)
p-p130Cas (Y410)
GAPDH
D
GE11
PEAK1 (Y635F)
PEAK1 (Y1188F)
PEAK1-KO
PEAK1-GFP
250
150
250
150
250
150
170
37
p-PEAK1 (Y635)
(Homemade)
Human PEAK1 (total)
(Cell Signaling)
GFP
Itg. b1
GAPDH
E
BioID
WCL
acatinib - 0.1 5 20 - 0.1 5 20
170
170
250
PEAK1
Itg.β1
pY
250
150
100
75
50
37
pY
40
GAPDH
70
p-Akt
40
GAPDH
F
GFP-TRAP
- 0.1 5
μM Saracatinib
250
250
250
p-PEAK1 (Y635)
pY
PEAK1 (total)
H
BioID
WCL
- 1 4 - 1 4 - 1 4
- - - + + + + + +
shRNA TNS3
Biotin
180
40
Talin1
GAPDH
G
Tensin-3 PEAK1
Tensin-3
PEAK1
DMSO
Saracatinib (5 μM)
I
PEAK1
Tensin-3
Actin
U251MG
+ shTNS3

Fig. S2. Biochemical and immunofluorescent analysis of Tensin3-PEAK1 interactions. (A) SW480 wild-type or PEAK1 KO (generated using CRISPR/Cas9) cells were lysed and analyzed by Western blot for PEAK1 expression. **(B)** SW480 PEAK1 KO cells stably expressing GFP-PEAK1 or GFP-PEAK1-Y635F cultured overnight on coverslips prior to fixation and staining for Tensin3; scale bar indicates 10 µm. **(C)** GE11 cells expressing GFP-PEAK1 were serum starved for 16h and treated with 50 ng/ml EGF for the indicated periods of time. Phosphorylation of indicated proteins was analyzed by Western blot. **(D)** Lysates of GE11 cells (GE11) and PEAK1-deficient GE11 cells (KO) reconstituted with GFP-PEAK1 (WT) or the GFP-PEAK1 mutants (Y635F) and (Y1188F) were analyzed by Western blot with antibodies against phospho-PEAK1 (Y365) (home-made), total PEAK1, GFP, β1 integrin, or GAPDH. **(E)** Representative Western blots of BioID assays performed using GE11/β1-BirA* cells treated with different concentrations of the Src inhibitor Saracatinib (AZD0530) for 24h. **(F)** GFP-PEAK1 was expressed in PEAK1-deficient GE11 cells and cells were treated with Saracatinib as indicated for 24h prior to cell lysis. Subsequently GFP pull downs were performed and PEAK1 Y635 phosphorylation was analyzed by Western blot. **(G)** U251MG cells spread on fibronectin-coated coverslips overnight with either Saracatinib (5 µM) or an equivalent volume of DMSO were fixed and stained for Tensin and PEAK1. Note the absence of PEAK1 from Tensin positive adhesion structures in Src inhibited cells. Scale bar indicates 10 µm. **(H)** Representative western blots of BioID assays performed using integrin β5-deficient U251MG cells expressing β5-BirA*, in which Tensin was depleted by two different shRNAs (1 and 4). Cells were treated with 50 µM biotin 24h before cell lysis. **(I)** U251MG cells transfected with control or shRNA against TNS3 were fixed and stained for PEAK1 and Tensin3. Note the lack of PEAK1 at cell-matrix adhesions in shTNS3 cells. Scale bar indicates 10 µm.

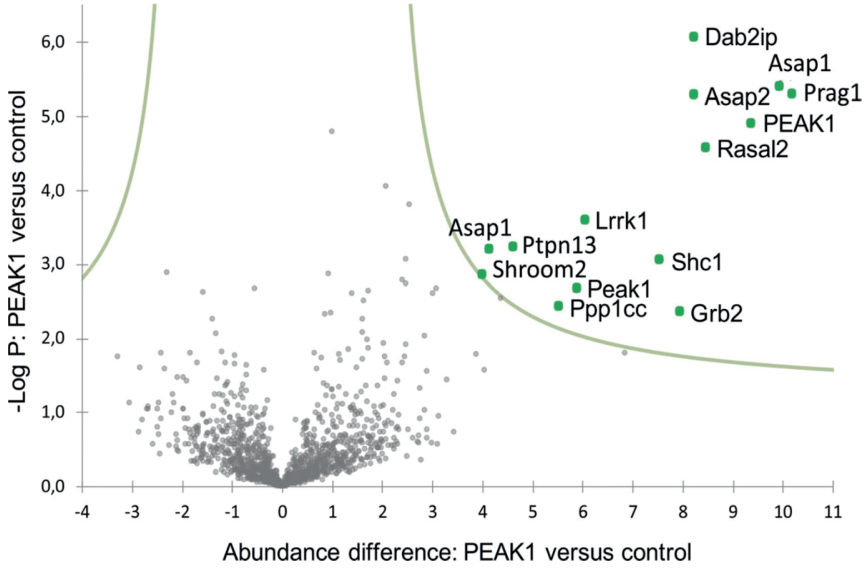

Fig. S3. PEAK1 interactome of EGF stimulated GE11 cells. PEAK1-deficient GE11 cells expressing GFP-PEAK1 were treated with EGF for 20 min, lysed, and subsequently subjected to immunoprecipitation using GFP-TRAP. Volcano plot shows proteins enriched in PEAK1-GFP over control (PEAK1 knockout cells) samples. The logarithmic ratio of proteins LFQs were plotted against negative logarithmic P values of a two-sided two samples t-test. The hyperbolic curve separates significantly enriched proteins (indicated in green) from common binders (FDR: 0.05, n=4).

SUPPLEMENTARY INFORMATION

Additional supplementary information is available online at https://rupress.org/jcb/article-abstract/221/8/e202108027/213273/PEAK1-Y635-phosphorylation-regulates-cell Tables S1, S2, S3, S4 and S5 are Excel files with the mass spectrometry data for proximity interactors of Integrin β1-BirA* (Table S1: complete data; S2: top 60 interactors), Integrin β3-BirA* (Table S3: complete data; S4: top 60 interactors), and GFP-Trap based affinity purification mass spectrometry of GFP-PEAK expressed in PEAK1-null GE11 cells (Table S5). Table S6 is a list of antibodies used in this study.